



HHS Public Access

Author manuscript

Oncogene. Author manuscript; available in PMC 2014 February 28.

Published in final edited form as:

Oncogene. 2013 August 29; 32(35): 4169–4180. doi:10.1038/onc.2012.418.

HER2 Stabilizes EGFR and Itself by Altering Autophosphorylation Patterns in a Manner That Overcomes Regulatory Mechanisms and Promotes Proliferative and Transformation Signaling

Zachary Hartman¹, Hua Zhao¹, and Yehenew M. Agazie^{1,2}

¹Department of Biochemistry, School of Medicine, West Virginia University, Morgantown, WV 26506

²The Marry Babb Randolph Cancer Center, School of Medicine, West Virginia University, Morgantown, WV 26506

Abstract

One of the causes of breast cancer is overexpression of the human epidermal growth factor receptor 2 (HER2). Enhanced receptor autophosphorylation and resistance to activation-induced down regulation have been suggested as mechanisms for HER2-induced sustained signaling and cell transformation. However, the molecular mechanisms underlying these possibilities remain incompletely understood. In the current report, we present evidence that show that HER2 overexpression does not lead to receptor hyper-autophosphorylation, but alters patterns in a manner that favors receptor stability and sustained signaling. Specifically, HER2 overexpression blocks EGFR tyrosine phosphorylation on Y1045 and Y1068, the known docking sites of c-Cbl and Grb2, respectively, while promoting phosphorylation on Y1173, the known docking site of the Gab adaptor proteins and phospholipase C gamma (PLC γ). Under these conditions, HER2 itself is phosphorylated on Y1221/1222, with no known role, and on Y1248 that corresponds to Y1173 of EGFR. Interestingly, suppressed EGFR autophosphorylation on the Grb2 and c-Cbl binding sites correlated with receptor stability and sustained signaling, suggesting that HER2 accomplishes these tasks by altering autophosphorylation patterns. In conformity with these findings, mutation of the Grb2 binding site on EGFR (Y1068F-EGFR) conferred resistance to ligand-induced degradation which in turn induced sustained signaling, and increased cell proliferation and transformation. These findings suggest that the Grb2 binding site on EGFR is redundant for signaling, but critical for receptor regulation. On the other hand, mutation of the putative Grb2 binding site in HER2 (Y1139) did not affect stability, signaling or transformation, suggesting that Y1139 in HER2 may not serve as a Grb2 binding site. In agreement with the role of EGFR in HER2 signaling, inhibition of EGFR expression reduced HER2-induced anchorage-independent

Users may view, print, copy, download and text and data- mine the content in such documents, for the purposes of academic research, subject always to the full Conditions of use: http://www.nature.com/authors/editorial_policies/license.html#terms

Address correspondence to: Yehenew M. Agazie, One Medical Center Drive, Department of Biochemistry, School of Medicine, West Virginia University, Morgantown, WV 26506, Phone: (304) 293-7756, Fax: (304) 293-6486, yagazie@hsc.wvu.edu.

The authors do not have any commercial affiliation or conflict of interest to disclose.

growth and tumorigenesis. These results imply that complementing HER2-targeted therapies with anti-EGFR drugs may be beneficial in HER2-positive breast cancer.

Keywords

HER2; EGFR; autophosphorylation; signaling; tumorigenesis

Introduction

The epidermal growth factor receptor (EGFR) family of receptor tyrosine kinases (RTKs) comprises four members that include EGFR1-4. The human counterparts are called HER1-4, also referred to as ErbB1-4 (1-3). All members are composed of an extracellular ligand-binding region, a transmembrane region, and a cytoplasmic region containing a Tyr kinase domain (except HER3) and Tyr autophosphorylation sites. Three of the family members, except HER2 (4), are activated by ligand binding (EGF, TGF α , heregulin, amphiregulin and heparin binding EGF) to the extracellular region, while HER2 is a constitutively active protein. Because EGFR1 is commonly known as EGFR and EGFR2 as HER2, we have used these abbreviations throughout this manuscript hereinafter.

The x-ray crystallographic structure of the EGFR ectodomain shows that the dimerization arm is autoinhibited in the resting state by intramolecular interaction between domains 2 and 4, but EGF binding induces conformational changes that relieve the dimerization arm, leading to homo- or heterodimerization (5-7). On the other hand, no interactions between domains 2 and 4 were observed in the HER2 ectodomain (4). As a result, HER2 can readily heterodimerize with ligand-activated family members or homodimerize with itself, especially under conditions of overexpression, a commonly encountered genetic abnormality particularly in breast cancer (8-11). It might be this structural property of HER2 that allows it to act as the preferred partner of heterodimerization with the other family members.

In the EGFR family, ligand activation leads to receptor dimerization and autophosphorylation of tyrosine residues in the C-terminal region that provide docking sites for Src homology 2 (SH2) or phosphotyrosine binding (PTB) domain-containing signaling molecules (12). These interactions lead to recruitment of adaptor proteins such as Grb2, Gab1/2 and Shc that mediate further interactions, translocation of enzymes to substrate micro domains such as PI3K and the Ras nucleotide exchange factor SOS, binding of regulatory proteins such as c-Cbl and RasGAP, and in some instances, activation of enzymes such as SHP1 and SHP2 (13-16). The formation of multiprotein signaling complexes at the level of the receptor accomplishes two major tasks - activation of mitogenic and cell survival signaling pathways, and down regulation of receptor activity (17-23).

Ligand binding to a receptor tyrosine kinase (RTK) induces endocytosis, ubiquitinylation and degradation, which is considered to be the primary mechanism of regulation. The EGFR family is also regulated by this mechanism (24-27), but HER2 seems to be a poorly regulated RTK even when it is heterodimerized with the other family members (28, 29). Although the ability of HER2 to overcome regulatory mechanisms is well recognized, the molecular mechanisms that enable HER2 to accomplish these tasks have remained

unexplored. In the current report, we present evidence that show that HER2 overcomes regulatory mechanism by altering autophosphorylation patterns both on itself and the heterodimerized EGFR in a manner that favors downstream signaling and disfavors ligand-induced down regulation. By doing so, HER2 exploits the EGFR to enhance its signaling, transformation, and tumorigenic potency.

Results

HER2 overexpression does not lead to receptor hyperphosphorylation

HER2 is a constitutively active protein (4), a property that may be key to its oncogenicity. We, therefore, evaluated receptor autophosphorylation patterns under conditions of HER2 overexpression. To address this question, it was necessary to ectopically express HER2 so that the impact of HER2 overexpression could be compared in the same cell line. Due to the significance of HER2 in breast cancer, we have used the non-tumorigenic MCF-10A breast epithelial and the BT20 breast cancer cell lines both of which express a “normal” amount of EGFR and a very low amount of endogenous HER2 and HER3 (30). We have also used the Skbr-3 breast cancer cell line that overexpress HER2, but has a “normal” level of EGFR to see if endogenously expressed EGFR and HER2 function cooperatively in cell transformation. For mechanistic studies involving mutant EGFR and HER2, the mouse embryo fibroblast (MEF) cells were used.

The pattern of EGF-induced total protein tyrosine phosphorylation in the presence and absence of HER2 expression was examined by immunostaining of total cell lysates with anti-pY (anti-phosphotyrosine) antibody. To examine the temporal dynamics of tyrosine phosphorylation, time-course EGF stimulation was employed. Surprisingly, the most significant differences were the initial hyperphosphorylation of the EGFR in the controls that rapidly declined after 10 minutes, and the relatively moderate, but sustained receptor autophosphorylation in the HER2 cells (Fig. S1A and B). Reprobing for EGFR showed that it was stabilized in the HER2 cells and rapidly degraded in the controls (Fig. S1A and B), which is consistent with previous reports (28, 29, 31). Further reprobing with anti-HER2 antibody revealed that HER2 was unaffected by ligand stimulation, confirming our recent report (30). These results suggest that receptor hyperphosphorylation occurs in the absence of HER2, but declines rapidly due to degradation.

The above findings led us concentrate on impact of HER2 overexpression on receptor autophosphorylation. EGFR and heterodimerized HER2 were isolated from cell lysates by immunoprecipitation reactions, and their total phosphorylation state was determined by immunostaining anti-pY antibody. To exclude differences due to ligand-induced receptor down regulation, the first 5 minutes of EGF stimulation was used for these experiments. Input total cell lysates used in these experiments had comparable amount of EGFR in all lanes, and similarly comparable levels of HER2 in the HER2 cells (Fig. 1A). Consistent with the results presented in Fig. S1A and B, EGF stimulation induced an enhanced receptor autophosphorylation in the controls, but a relatively modest autophosphorylation in the HER2 cells (Fig. 1B). Significant receptor autophosphorylation also occurred in the HER2 cells in the absence of EGF stimulation, suggesting that HER2 can induce basal signaling under conditions of overexpression. Successive reblotting showed that EGFR was efficiently

precipitated, and the ectopically expressed HER2 was likewise co-precipitated with EGFR mainly in EGF-stimulation dependent manner. Band density measurements from at least three independent experiments showed that EGF-induced total receptor autophosphorylation was lower by approximately 25% in the HER2 cells (Fig. 1C). This looked paradoxical, but it nevertheless provided a clue as to the occurrence of reduced receptor autophosphorylation when HER2 is co-expressed with the EGFR.

HER2 alters autophosphorylation patterns in a manner that confers differential interaction

The unexpected differences in total receptor autophosphorylation between the controls and the HER2 cells led us investigate the phosphorylation state of individual autophosphorylation sites in both EGFR and HER2 in total cell lysates whose input protein levels are shown in Fig. 2A. EGF stimulation led to a robust phosphorylation of the EGFR on Y1045 and Y1068, the docking sites of c-Cbl and Grb2, respectively, in the controls, but phosphorylation on these sites was significantly reduced in the HER2 cells (Fig. 2B). In addition, phosphorylation on Y1148, the docking site of the Shc proteins, was lower in the HER2 cells, although not as dramatic as the Grb2 and the c-Cbl sites. On the other hand, phosphorylation on Y1173, the docking site of Gab1 and PLC γ , was significantly higher in the HER2 cells and lower in the controls. We were also able to determine the state of HER2 autophosphorylation on Y1221/1222, which have no corresponding sites in EGFR, and on Y1248 that corresponds to Y1173 of EGFR. HER2 was phosphorylated even in the absence of EGF stimulation on these sites, which was further enhanced by EGF stimulation. These findings demonstrate that EGFR autophosphorylation is enhanced on the Gab1 (which recruits PI3K and SHP2) and PLC γ binding sites, and suppressed on the c-Cbl and the Grb2 binding sites in the presence of HER2.

The observed differential autophosphorylation pattern could have been due to activation of certain phosphotyrosyl phosphatases (PTPs) by HER2. To verify this point, cells were treated with the general PTP inhibitor orthovanadate and lysates prepared from them were analyzed in the same way as above. Inhibition of PTP activity both in the control and HER2 cells derive from the MCF-10A and BT20 lines did not lead to changes in autophosphorylation patterns (Fig. 2C and data not shown). Therefore, the reduced total receptor autophosphorylation in the HER2 cells was due to altered autophosphorylation induced by HER2.

Since altered autophosphorylation might lead to differential interaction with downstream signaling proteins, immunoprecipitation experiments were conducted to test this possibility. Consistent with the autophosphorylation data, the EGF-induced interaction of c-Cbl and Grb2 proteins with EGFR was elevated in the controls and lowered in the HER2 cells (Fig. 2D), while the reverse was true for Gab1, p85 (subunit of PI3K) and SHP2. Despite moderate differences in EGFR phosphorylation on Y1148 between the control and the HER2 cells, the interaction of the Shc proteins was significantly lower in the HER2 cells. This outcome might reflect additive effects - directly due to reduced pY1148 and indirectly due to reduced pY1068 (Grb2-mediated); note that Shc proteins can make direct and indirect (through Grb2) interactions with activated receptors. Therefore, HER2 promotes altered autophosphorylation that leads to differential interaction with signaling and regulatory

proteins. Although we have not directly tested HER2 autophosphorylation at the corresponding Grb2 (Y1139) and c-Cbl (Y1112) binding sites due to lack of specific antibodies, the low level of Grb2 and c-Cbl interaction in the HER2 cells suggests that HER2 may not be phosphorylated on these sites.

c-Cbl is unable to interact with the EGFR:HER2 heterodimer, leading to reduced ubiquitinylation

A previous study has shown that controlled EGFR:HER2 heterodimers tend to exclude c-Cbl interaction (32), but the mechanism was not known. The results presented in Figs. 2B and C demonstrated that autophosphorylation of the EGFR and possibly HER2 on the c-Cbl and the major Grb2 binding sites is very low in the presence of HER2, eliminating the direct and indirect interaction of c-Cbl. This may be the mechanism by which HER2 excludes c-Cbl. Consistent with this notion EGFR coprecipitated with c-Cbl efficiently in the controls, and poorly in the HER2 cells (Fig. 3A and B). Furthermore, HER2 was undetectable in c-Cbl immunoprecipitates, confirming that c-Cbl does not interact with EGFR-HER2 heterodimers. Reprobing with anti-c-Cbl antibody showed that the amount of c-Cbl was comparable in all lanes. These results, together with the findings in Fig. 2B and D, show that the mechanism by which HER2 excludes the interaction of c-Cbl is through suppression of autophosphorylation on the direct and indirect c-Cbl binding sites.

Based on the results in Fig. 3A and B, it was reasoned that exclusion of c-Cbl interaction by HER2 could lead to inhibition of ubiquitinylation. Consistent with this assumption, EGFR in the control cells was highly ubiquitinylated, but less so in the HER2 cells despite the presence of comparable amount of receptor molecules in all lanes (Fig. 3C and D). Therefore, the mechanism by which HER2 protects itself as well as EGFR from ligand-induced ubiquitinylation and degradation is by regulating the interaction of c-Cbl through altering autophosphorylation patterns.

HER2-induced inhibition of Grb2-binding site autophosphorylation does not perturb signaling

Inhibition of EGFR autophosphorylation on Y1068 in the HER2 cells was unexpected as this site was previously reported to promote Ras activation by acting as the major Grb2-SOS complex docking site. We therefore tested the state of EGF-induced downstream signaling under our experimental conditions. Because HER2 is known to induce sustained signaling, these experiments were conducted in a time course fashion. ERK1/2 and Akt activation was sustained in the HER2 cells and short-lived in the controls, suggesting the existence of an inverse relationship with elevated phosphorylation of the Grb2 binding site in EGFR (Fig. 4A and D). In agreement with the dynamics of EGF-induced EGFR degradation (Fig. S1 and (30)), initial ERK1/2 and Akt activation (first 10 minutes) was comparable in both the controls and the HER2 cells, but rapidly declined in the former and sustained in the latter. It was also possible to discern a revamping pattern in ERK1/2 and Akt activation in the HER2 cells after 2 hours, reflecting receptor recycling as reported by us recently (30). As compared to the controls, the HER2 cells showed basal ERK1/2 and Akt activation, suggesting that HER2 alone can induce a low level of constitutive signaling. Anti-panERK2 immunostaining showed that the amount of total protein loaded to each lane was

comparable. Band density measurements (Fig. 4B, C, E and F) confirmed that ERK1/2 and Akt activation in both cells were comparable at the 10 minutes time point, but rapidly declined in the controls to approximately 20% of the initial value, and never fell below 50% of the initial value in the HER2 cells. Therefore, the low level of Grb2 binding-site autophosphorylation in the presence of HER2 does not perturb signaling.

Y108F-EGFR induces sustained signaling compared to the wild-type counterpart

The induction of sustained signaling by HER2 while suppressing Grb2 binding required direct testing. Site-directed mutagenesis was used to replace Y1068 in EGFR and Y1139 in HER2 with Phe, which were referred to as Y1068F-EGFR and Y1139F-HER2, respectively. The vector, the wild-type and the mutant proteins (FLAG-tagged at the c-terminus) were expressed by retrovirus transduction in the mouse embryo fibroblast (MEF) cells that have very low-to-undetectable level of endogenous EGFR and HER2. Time-course EGF stimulation studies were conducted to examine the impact of the Grb2 binding-site mutation on the signaling and dynamics of ligand-induced receptor regulation. Expression of both WT-EGFR and Y1068F-EGFR led to an enhanced ERK1/2 and Akt activation initially, but it was short lived in the WT-EGFR and sustained in the Y1068F-EGFR cells (Fig. 5A). Anti-EGFR immunostaining revealed that Y1068F-EGFR was resistant to EGF-induced degradation, but the wild type counterpart was not. With regard to HER2, both WT-HER2 and Y1139F-HER2 were able to induce sustained ERK1/2 and Akt activation, which was slightly enhanced by EGF stimulation (Fig. 5B). Reprobing for HER2 showed that both the WT-HER2 and the Y1139F-HER2 proteins were unaffected by EGF stimulation. Hence, Y1139, the putative Grb2 binding site in HER2, does not seem to play any significant role either in mediating signaling or receptor down regulation.

The above results led us determine the state of Grb2, SOS and c-Cbl interaction with the wild-type and the mutant EGFR proteins by immunoprecipitation experiments. As expected, mutation of the Grb2 binding site significantly reduced the interaction of Grb2 and SOS with EGFR (Fig. 5C). The interaction of c-Cbl was very low in the Y1068F-EGFR cells regardless of the presence of intact Y1045, suggesting that the Grb2-mediated (indirect) interaction plays a major role in recruiting c-Cbl to EGFR. Consistent with loss of c-Cbl interaction, Y1068F-EGFR was less ubiquitinated than the wild type counterpart. Reprobing for EGFR showed that comparable amount of both WT-EGFR and Y1068F-EGFR were present in all lanes. These findings suggest that Grb2 mediates receptor ubiquitinylation and degradation by acting as an adaptor to c-Cbl. In support of our conclusion, previous reports have also shown that Grb2 mediates receptor degradation by recruiting c-Cbl (33, 34). Therefore, HER2-induced suppression of EGFR autophosphorylation at the Grb2 binding site protects EGFR from ligand-induced degradation, and affords the EGFR with the ability to induce sustained signaling.

EGF-induced Y1068F-EGFR trafficking resembles that of WT-EGFR in presence of HER2

The resistance of Y1068F-EGFR to ligand-induced degradation was very similar to that induced by HER2 coexpression (Fig. S1A and B, (30)). To further compare this possibility, the dynamics of ligand-induced EGFR trafficking was studied by fluorescence microscopy in MEF cells ectopically expressing WT-EGFR or Y1068F-EGFR, and in BT20 and in

MCF-10A cells expressing vector alone or HER2. Cells were treated with TRITC-EGF at 4°C to initiate binding without inducing internalization, hence allowing a synchronized endocytosis and processing when cells are transferred back to 37°C after removal of unbound EGF (35). Both WT-EGFR and Y1068F-EGFR expressed in MEFs were at the plasma membrane when cells were fixed immediately, but incubation at 37°C led to internalization within 10 minutes (Fig. 5D). Similarly, EGFR in both the control and the HER2 cells derived from the BT20 and the MCF-10A lines was at the plasma membrane at the zero time point, but was readily internalized within 10 minutes of incubation at 37°C as depicted by speckled cytoplasmic distribution (Fig. 5E and F). Upon further incubation, ectopically expressed WT-EGFR in the MEFs, and endogenous EGFR in the control BT20 and MCF-10A cells was sorted to the perinuclear region and decayed gradually. On the other hand, Y1068F-EGFR in the MEFs behaved like WT-EGFR in the HER2 cells; in these cells, most of the EGFR signal was sorted to one side of the nucleus with gradual outward extension and minimal decline. Therefore, the dynamics of EGF-induced Y1068F-EGFR processing resembles HER2 overexpression-induced EGFR recycling.

Y1068F-EGFR is more transforming when compared to the wild-type counterpart

The results presented in Fig. 5 demonstrated that the Y1068F-EGFR is more signaling competent than the wild type counterpart, while both the wild type and the mutant HER2 proteins are equally competent. The biological significance of these observations was further tested by evaluating changes in cell morphology, growth and transformation. In the absence of EGF stimulation, neither the wild-type nor the mutant EGFR protein induced any appreciable change in cell morphology, proliferation or transformation (data not shown). In the presence of EGF (2 ng/ml), however, the distinctive properties of the two proteins became apparent. MEFs expressing the Y1068F-EGFR acquired an elongated and refractive morphology in 2D (Fig. S2A), an increased proliferative potential (Fig. 6A, left) and ability to form colonies in soft agar (Fig. 6B). On the other hand, the mere expression of both WT-HER2 and Y1139F-HER2 proteins induced morphological changes characterized by an interspersed and refractive appearance that forms foci-like structures de novo (Fig. S2B). In addition, both HER2 proteins were capable of inducing increased cell proliferation (Fig. 6A, right), and robust colony formation in soft agar (Fig. 6C). These results suggest that Y1068F-EGFR is superior in inducing cell growth and transformation than its wild type counterpart, which in turn suggests that inhibition of EGFR phosphorylation on Y1068 by HER2 confers signaling and transformation efficiency. Furthermore, these data show that mutation of Y1139 in HER2, the putative Grb2-binding autophosphorylation site, does not perturb transforming ability, suggesting that Y1139 in HER2 may not play any significant role. Overall, the superiority of HER2 in inducing enhanced cell growth and transformation suggests that it has additional effects other than altering autophosphorylation patterns.

To further corroborate the role of EGFR in HER2-induced transformation, its expression was silenced in the Skbr-3 breast cancer cell line that naturally has amplified HER2 gene and normal level of EGFR. Silencing EGFR in these cells reduced the size of HER2-induced colony growth in 3D without significantly affecting colony number (Fig. 6D-F). These results confirm the ectopic HER2 overexpression data in the BT20 and the MCF-10A cells that EGFR contributes significantly to HER2-induced signaling and transformation.

HER2 exploits the EGFR to enhance its tumorigenic potential

The results so far described demonstrate that HER2 alters autophosphorylation patterns to confer resistance to ligand-induced degradation and to ultimately enhance cooperative signaling and transformational capacity. Finally, we sought to test whether or not the normally-expressed EGFR contributes significantly to HER2-induced tumorigenesis *in vivo*.

The BT20 HER2 cells expressing control or anti-EGFR shRNA were injected subcutaneously into nude mice, and tumor formation was monitored by visual observation. The HER2 cells in which EGFR expression was silenced formed smaller and rounded tumors, while those that co-expressed EGFR with HER2 formed larger and irregular ones (Fig. 6G). Pictures of isolated tumors further showed differences in tumor size and shape (Fig. 6H). Measuring tumor weight confirmed that blocking EGFR expression in the HER2 cells reduced tumor burden by approximately 3.5 fold (Fig. 6I). Therefore, HER2-induced tumorigenesis is dependent on EGFR, suggesting that the normally-expressed EGFR may potentiate the oncogenic property of HER2 in HER2-positive breast cancer. In other words, HER2 is capable of mustering signaling efficiency from the normally expressed family members by promoting their stability through altering autophosphorylation patterns.

Discussion

HER2 is an oncogenic transmembrane tyrosine kinase that induces cell transformation and tumorigenesis when it is overexpressed in tissues. Its overexpression, primarily due to gene amplification, is one of the major causes of breast cancer. HER2 is a constitutively active protein (4) with intrinsically low tyrosine kinase activity (36, 37). This property of HER2 may be responsible for its ability to escape activation-induced down regulation, one of the suggested mechanisms for its oncogenesis. We thus investigated the effect of HER2 overexpression on receptor autophosphorylation and its impact on protein stability, downstream signaling, and cell transformation. Furthermore, we have presented data that show that EGFR contributes significantly to HER2-induced tumorigenesis in xenograft mice models.

We have shown that HER2 overexpression leads neither to increased overall cellular tyrosine phosphorylation nor to receptor hyper-autophosphorylation. To the contrary, receptor hyper-autophosphorylation occurs in the absence of HER2 (Fig. 1B and C). These data were indicative of the occurrence of reduced receptor autophosphorylation when EGFR and HER2 heterodimerize. Analyzing specific autophosphorylation sites demonstrated that phosphorylation of the EGFR on Y1045 and Y1068 (the docking sites of c-Cbl and Grb2, respectively) was suppressed in the absence of HER2 while the opposite was true for Y1173 of EGFR and for Y1221/1222 and Y1248 of HER2 (Fig. 2B). Although we have not determined phosphorylation of the putative c-Cbl and Grb2 docking sites (Y1112 and Y1139, respectively) in HER2 due to lack of specific antibodies, the modest overall autophosphorylation suggests that phosphorylation on these sites may not occur.

In agreement with the autophosphorylation data, c-Cbl and Grb2 interact strongly with EGFR homodimers, and poorly with EGFR:HER2 heterodimers (Fig. 2D). The poor interaction of c-Cbl and Grb2 with HER2-containing complexes provides further evidence

that HER2 may not be phosphorylated on Y1112 and Y1139. The low level of c-Cbl binding-site autophosphorylation in the presence of HER2 lends mechanistic support to the previous observation that EGFR:HER2 complexes tend to exclude c-Cbl binding (32). In addition to its signaling role, Grb2 is known to mediate the interaction of c-Cbl with activated receptor molecules (34). Hence, the low level of Y1068 phosphorylation in the presence of HER2 blocks the indirect interaction of c-Cbl (Fig. 2D, and Fig. 3A and B), which in turn leads to the low level of receptor ubiquitinylation (Fig. 3C and D). Therefore, the mechanism by which HER2 confers receptor stability is through altered autophosphorylation. However, our results cannot exclude the existence of other as yet unidentified ubiquitin ligases excluded by HER2 that may contribute to receptor resistance to ligand-induced degradation.

While blocking autophosphorylation on the c-Cbl and the Grb2 binding sites, HER2 promotes EGFR phosphorylation on Y1173 and its own phosphorylation on Y1248 and Y1221/1222 (Fig. 2B). Phosphorylated Y1173 of EGFR and Y1248 of HER2 are known docking sites for the Gab1/Gab2 adaptor proteins (38, 39). Consistent with the phosphorylation data, the interaction of Gab1 was elevated in the HER2 cells, and lowered in the control cells (Fig. 2D). Upon binding to RTKs and phosphorylation on multiple tyrosine residues, Gab1 serves as a docking platform for several signaling proteins, leading to formation of multiprotein complexes. Because EGFR and HER2 lack tyrosine residues that mediate direct PI3K binding, the interaction of PI3K with the EGFR:HER2 complexes is most probably through Gab1. Previous reports suggest that SHP2, the known positive effector of EGFR and HER2 signaling, interacts with EGFR and HER2 through Gab1 (40, 41). Therefore, the increased interaction of SHP2 with EGFR and HER2 complexes may as well be through Gab1.

HER2 does not significantly influence the state of EGFR phosphorylation on Y1148, the docking site of the Shc adaptor proteins, but relatively less Shc proteins bind to EGFR:HER2 heterodimers. The reduced Shc interaction may be related to low Grb2 binding in the HER2 cells; note that Shc proteins are known to also make indirect interaction with RTKs through Grb2 (42, 43). Hence, the low level of EGFR autophosphorylation on Y1068 in the presence of HER2 reduces the interaction of Grb2 directly and that of c-Cbl and Shc proteins indirectly. A previous phosphoproteomic study suggested that Y1222 in HER2 may mediate Shc binding (44), but our results demonstrate very low binding of Shc proteins regardless of enhanced HER2 phosphorylation on Y1221/1222. It is possible that HER2 molecules behave differently inside (this report) and outside (44) the cell. Nonetheless, the presence of HER2 autophosphorylation on these sites suggests that they may contribute to the direct and indirect binding of other signaling proteins. It will be interesting to address these points in future studies. Overall, our results show that HER2 alters autophosphorylation patterns of the EGFR and of itself, favoring Gab1, p85 (PI3K) and SHP2, and disfavoring c-Cbl and Grb2 interactions.

The mechanism by which HER2 alters the autophosphorylation pattern within the heterodimer is unknown at this stage. Recent structural and modeling studies on receptor tyrosine kinases suggest that the kinase domains of dimerized receptor molecules form an asymmetric dimer that has a positive allosteric effect on kinase activation (45, 46). This

has been demonstrated for EGFR homodimers, FGFR1 homodimers, FGFR2 homodimers, and HER2 and HER4 heterodimers. The occurrence of such kinase domain asymmetry in the EGFR:HER2 heterodimer has not been demonstrated, but it is thought to be a common phenomenon (47). It is possible that subtle structural arrangements in the EGFR:HER2 heterodimer hinder phosphorylation on the direct and indirect c-Cbl interaction sites, while promoting on those sites that mediate downstream signaling. A second possibility is that the kinase domain of HER2 may have the ability to discriminate among autophosphorylation sites, leading to distinctive autophosphorylation. A third possibility might be that the intrinsically low tyrosine kinase activity of HER2 (36, 37) may lead to phosphorylation of some, but not all sites on EGFR and HER2 itself, leading to differential autophosphorylation patterns. Future structural studies on EGFR:HER2 heterodimers may be needed to delineate between these possibilities.

Because HER2 promotes the interaction of the SHP2 tyrosine phosphatase, the known positive effector of RTK signaling, including EGFR and HER2, one may also argue that HER2 suppresses autophosphorylation on the c-Cbl and Grb2 binding sites indirectly by facilitating SHP2-mediated dephosphorylation. However, this possibility is unlikely since SHP2 is a highly selective phosphatase, targeting only RasGAP docking sites in EGFR (17) and HER2 (48). The involvement of other PTPs also is unlikely since treatment with orthovanadate, the general PTP inhibitor, did not lead to differences in the autophosphorylation patterns (Fig. 2C). In addition, the occurrence of this event in less than 2 minutes of EGF stimulation strengthens the notion that HER2 does not act through tyrosine phosphatases to modulate autophosphorylation patterns.

One of the most unexpected findings was the induction of sustained signaling by the EGFR mutant lacking the Grb2 binding site (Y1068F-EGFR) (Fig. 5A). Analysis of EGF-induced receptor regulation has revealed that Y1068F-EGFR is relatively resistant to degradation. Immunoprecipitation studies further revealed that EGFR lacking the Grb2 binding site interacts poorly with c-Cbl and is least ubiquitinated (Fig. 5C), explaining the observed resistance to ligand-induced degradation. A further layer of evidence came from fluorescent-tagged EGF stimulation studies which demonstrated that Y1068F-EGFR is efficiently internalized upon EGF stimulation, but not degraded. Hence, the sustained signaling efficiency of the Y1068F-EGFR is related to its resistance to EGF-induced degradation. Comparison of ligand-induced Y1068F-EGFR sorting with HER2-induced sorting of endogenous EGFR (compare Fig. 5D with E and F) showed a striking similarity, providing experimental evidence for the HER2-induced suppression of EGFR autophosphorylation on Y1068 conferring resistance to ligand-induced degradation. The increased cell proliferation and transformation induced by the Y1068F-EGFR (Fig. 6A and B) provide further support for this role of HER2.

The commonly-held notion is that Grb2 mediates Ras activation by acting as an adaptor to the nucleotide exchange factor SOS to bind to activated receptor tyrosine kinases at the plasma membrane where functional Ras resides. The finding that HER2 efficiently activates the Ras-ERK signaling pathway while suppressing Grb2 interaction contrasts with this notion. The ability of the Y1068F-EGFR to induce enhanced and sustained ERK1/2 and Akt activation, while having significantly reduced Grb2-SOS binding confirms the current

findings. The corresponding HER2 mutant (Y1139F-HER2) that lacks Grb2 binding site also signals as efficiently as the wild-type counterpart. Therefore, interaction of SOS with activated RTKs through Grb2 to activate Ras may be redundant or dispensable. In fact, the current data suggest that the major role of Grb2 bound to pY1068-EGFR is to mediate a receptor regulatory loop by coordinating the interaction of c-Cbl. A recent study suggested that the ERM proteins (ezrin, radixin, moesin) may play critical role in recruiting SOS to Ras (49), which may also be functional in HER2 signaling. Future studies are needed to further elucidate how HER2 activates the Ras-ERK signaling pathway without utilizing Grb2.

Conferring receptor resistance to activation-induced down regulation through modulation of receptor autophosphorylation patterns seems to be the mechanism for HER2 in promoting sustained signaling and cell transformation. The results presented in the current report (Fig. 6D–I) reveal that maximal transformation and tumorigenesis by HER2 was dependent on EGFR. Loss of EGFR expression abolished HER2-induced anchorage-independent growth by the HER2 amplified breast cancer cell line. Furthermore, the enhanced tumor growth induced by HER2 overexpression in the BT20 breast cancer cell line was significantly suppressed, suggesting that HER2 exploits the normally expressed EGFR to maximize its oncogenicity. Based on ³H-thymidine-incorporation experiments (50), it was previously suggested that EGFR is not required for HER2-induced cell proliferation which is in contrast to our findings. It may be necessary to determine the significance of EGFR in HER2-induced transformation using transformation and *in vivo* studies in the future. Nonetheless, the implication of our findings is that complementing HER2-targeted therapies with anti-EGFR drugs may be beneficial in HER2-positive breast cancer as also evidenced by recent clinical trials where the dual tyrosine kinase inhibitor lapatinib was demonstrated to provide clinically beneficial results when administered in combination with anti-HER2 drugs such as herceptin (51).

Materials and Methods

Cells, cell culture and reagents

The cells used in this study, the MCF10A breast epithelial, and the BT20 and the Skbr-3 breast cancer cell lines, were purchased from ATCC, while the mouse embryo fibroblasts (MEFs) were a gift from Dr. Steven Frisch (West Virginia University). The MEFs and the BT20 cells were grown in regular Dulbecco's Modified Eagle's Medium (DMEM) supplemented with 10% fetal calf serum, while the MCF10A were grown in DMEM supplemented with the indicated ingredients (10 µg/ml recombinant human insulin, 20 ng/ml EGF (PeproTech), 0.5 µg/ml hydrocortisone, 100 ng/ml cholera toxin (Sigma) and 5% horse serum), as described previously (52). All cell lines were grown in a 37°C incubator with 5% CO₂ supply. The anti-EGFR polyclonal antibody (E1157), and the anti-FLAG (F3165) and the anti-β-actin (A5441) monoclonal antibodies were purchased from Sigma-Aldrich, while the anti-HER2 (610162) monoclonal antibody was from Pharmagen. Antibodies to phospho-ERK1/2 (9101S), phospho-Akt (9271S), phospho-EGFR (2234, 2237, 4404, 4407) and phospho-HER2 (2243, 2244) were from Cell Signaling. The anti-c-CBL antibodies (SC-170 and SC-1651) and the anti-panERK2 antibody (SC-81457) were bought from Santa Cruz

Biotechnology. Secondary antibodies conjugated with horseradish peroxidase were from Amersham (NA934V and NA931V), and Molecular Probes (A11079). TRITC-labeled EGF was purchased from Molecular Probes.

Subcloning, retroviral transduction and production of stable cell lines

Full-length wild type and mutant HER2 and EGFR proteins were subcloned into the REBNA/IRES/GFP retroviral vector as reported previously (53). Recombinant retroviral particles expressing the different HER2 and EGFR proteins were produced by transfection into appropriate packaging cells using the FuGENE 6 transfection reagent (Roche). The MCF-10A, the BT20 and the MEF cell lines stably expressing the vector and the different EGFR and HER2 proteins were produced by infection with the respective retroviruses in the presence of 1 μ g/ml polybrene (Sigma). After incubation in growth medium for approximately 48 hours, cells were treated with 1 μ g/ml blasticidine, the selection antibiotic expressed by the viral vector, to remove non-expressing cells. Blasticidine-resistant cell populations were used for the various experiments described in this manuscript.

Stable anti-EGFR shRNA expression

The expression of the EGFR in the HER2 cells derived from the BT20 line was accomplished as described by us and others (54). Briefly, double-stranded DNA the codes for anti-EGFR shRNA was custom-synthesized (Integrated DNA Technologies) and ligated into the BamHI and EcoRI sites of pSIREN-RetroQ-TetP (BD Biosciences, Palo Alto, CA). The targeting oligonucleotide sequence was 5'-GGAGCTGCCCATGAGAAAT-3'. After packaging in appropriate cells, transient supernatants (after 48 hours of incubation) were used to infect the BT20-HER2 and the Skbr-3 cells. A non-targeting anti-Luciferase shRNA was used as a control. Non-expressing cells were removed by puromycin treatment, and resistant populations were used for the in vivo Xenografting studies described in Fig. 7.

Preparation of cell lysates, gel electrophoresis and immunostaining analysis

All cell lysates were prepared in a buffer containing 20 mM Tris-HCl, pH7.2, 150 mM NaCl, 50 mM NaF, 1 mM EDTA, 10% glycerol, 1% triton-X-100, 1 mM sodium orthovanadate and a protease inhibitor cocktail. Lysates were briefly sonicated to breakdown chromosomal DNA that could interfere with protein separation by polyacrylamide gel electrophoresis. After clearing by centrifugation at 12,000 rpm for 10 minutes, the lysates were analyzed as described in the respective experiments. For separation of proteins, samples were mixed with Laemmli sample buffer, denatured by boiling for 10 minutes, and then run on an 8% or 10% denaturing polyacrylamide gel. After transfer onto a nitrocellulose membrane and blocking with 3% bovine serum albumin, the membranes were stained with primary antibodies overnight at 4°C, washed 3 times with TBST (Tris-buffered saline containing 0.1% Tween-20) to remove unbound primary antibody, stained with secondary antibodies for 1 hour at room temperature, washed 3 times with TBST to remove unbound secondary antibody, and finally detected by the chemiluminescence method.

Immunoprecipitation studies

Cells expressing vector alone or WT-HER2 were grown to about 80% density, serum starved overnight, and stimulated with 10 ng/ml EGF for desired time points. Lysates prepared from these cells were first cleared by centrifugation at 12,000 rpm, and then subjected to immunoprecipitation with respective antibodies at 4°C overnight. Precipitates were captured on protein A/G sepharose beads by further incubation for 1 hour. Finally, precipitates were washed three times with lysis buffer and then eluted by addition of Laemmli sample buffer and boiling for 10 minutes at 100°C. Eluted proteins were separated on polyacrylamide gel electrophoresis and processed for immunostaining as described above.

Anchorage-independent growth assay

Anchorage-independent growth in soft agar was performed in 6 cm cell culture plates. After covering bottom of plates with 0.3% agar in the growth medium, approximately 10^5 cells suspended in 3 ml of growth medium and mixed with melted agar to a final concentration of 0.3% were immediately poured onto the agar overlay. The agar cultures were transferred to a 37 °C and 5% CO₂ incubator and maintained for 15 days. The cells were fed with growth medium containing 0.3% soft agar twice, and after that, feeding was by replenishing DMEM supplemented with 10% fetal bovine serum. Colony formation was monitored by visualization under a microscope, and pictures were taken using an Olympus IX71 microscope equipped with DP30BW digital camera.

TRITC-labeled EGF studies

Cover slips for TRITC-labeled EGF fluorescence studies were prepared as described previously (18, 35, 55). Cells grown on cover slips, serum-starved overnight, pre-chilled at 4°C for 1 hour, treated with 10 ng/ml TRITC-labeled EGF for under chilled conditions, washed twice with ice-cold serum-free DMEM, replenished with the same serum-free medium and incubated at 37°C for the desired time points. Cover slips were then rinsed with room temperature PBS, fixed in 4% paraformaldehyde for 20 minutes, washed 3 times with PBS, and mounted on microscopic slides. Pictures were collected using the 40× objectives of Olympus IX-71.

In vivo tumorigenesis studies

Female nude mice were purchased from Jackson laboratories. Approximately 10^6 MCF-10A-HER2 cells expressing control or anti-EGFR shRNA were mixed 1:1 with matrigel (BD Biosciences) and injected subcutaneously into the rump region of each mouse; three mice were used in each group. Tumor growth was monitored by visual observation. When the control shRNA-HER2 mice developed tumors that were 1 cm in diameter, all mice were sacrificed, pictures collected, tumors retrieved and their weights measured.

Supplementary Material

Refer to Web version on PubMed Central for supplementary material.

Acknowledgments

This work was supported by a grant number CA124940 from the National Cancer Institute (NCI), a component of the National Institute of Health (NIH) to YMA.

References

1. Dionne CA, Jaye M, Schlessinger J. Structural diversity and binding of FGF receptors. *Ann N Y Acad Sci.* 1991; 638:161–6. [PubMed: 1664682]
2. Johnson DE, Williams LT. Structural and functional diversity in the FGF receptor multigene family. *Adv Cancer Res.* 1993; 60:1–41. [PubMed: 8417497]
3. Ullrich A, Coussens L, Hayflick JS, Dull TJ, Gray A, Tam AW, et al. Human epidermal growth factor receptor cDNA sequence and aberrant expression of the amplified gene in A431 epidermoid carcinoma cells. *Nature.* 1984 May-Jun;309(5967):418–25. [PubMed: 6328312]
4. Garrett TP, McKern NM, Lou M, Elleman TC, Adams TE, Lovrecz GO, et al. The crystal structure of a truncated ErbB2 ectodomain reveals an active conformation, poised to interact with other ErbB receptors. *Mol Cell.* 2003 Feb; 11(2):495–505. [PubMed: 12620236]
5. Ferguson KM, Berger MB, Mendrola JM, Cho HS, Leahy DJ, Lemmon MA. EGF activates its receptor by removing interactions that autoinhibit ectodomain dimerization. *Mol Cell.* 2003 Feb; 11(2):507–17. [PubMed: 12620237]
6. Garrett TP, McKern NM, Lou M, Elleman TC, Adams TE, Lovrecz GO, et al. Crystal structure of a truncated epidermal growth factor receptor extracellular domain bound to transforming growth factor alpha. *Cell.* 2002 Sep 20; 110(6):763–73. [PubMed: 12297049]
7. Ogiso H, Ishitani R, Nureki O, Fukai S, Yamanaka M, Kim JH, et al. Crystal structure of the complex of human epidermal growth factor and receptor extracellular domains. *Cell.* 2002 Sep 20; 110(6):775–87. [PubMed: 12297050]
8. Badache A, Goncalves A. The ErbB2 signaling network as a target for breast cancer therapy. *J Mammary Gland Biol Neoplasia.* 2006 Jan; 11(1):13–25. [PubMed: 16947083]
9. Carlsson J, Nordgren H, Sjostrom J, Wester K, Villman K, Bengtsson NO, et al. HER2 expression in breast cancer primary tumours and corresponding metastases. Original data and literature review. *Br J Cancer.* 2004 Jun 14; 90(12):2344–8. [PubMed: 15150568]
10. Fukushige S, Matsubara K, Yoshida M, Sasaki M, Suzuki T, Semba K, et al. Localization of a novel v-erbB-related gene, c-erbB-2, on human chromosome 17 and its amplification in a gastric cancer cell line. *Mol Cell Biol.* 1986 Mar; 6(3):955–8. [PubMed: 2430175]
11. King CR, Kraus MH, Aaronson SA. Amplification of a novel v-erbB-related gene in a human mammary carcinoma. *Science.* 1985 Sep 6; 229(4717):974–6. [PubMed: 2992089]
12. Pawson T, Gish GD. SH2 and SH3 domains: from structure to function. *Cell.* 1992; 71(3):359–62. [PubMed: 1423600]
13. Feng GS, Shen R, Heng HH, Tsui LC, Kazlauskas A, Pawson T. Receptor-binding, tyrosine phosphorylation and chromosome localization of the mouse SH2-containing phosphotyrosine phosphatase Syp. *Oncogene.* 1994; 9(6):1545–50. [PubMed: 8183548]
14. Hadari YR, Kouhara H, Lax I, Schlessinger J. Binding of Shp2 tyrosine phosphatase to FRS2 is essential for fibroblast growth factor-induced PC12 cell differentiation. *Mol Cell Biol.* 1998; 18(7):3966–73. [PubMed: 9632781]
15. Lechleider RJ, Sugimoto S, Bennett AM, Kashishian AS, Cooper JA, Shoelson SE, et al. Activation of the SH2-containing phosphotyrosine phosphatase SH-PTP2 by its binding site, phosphotyrosine 1009, on the human platelet-derived growth factor receptor. *J Biol Chem.* 1993; 268(29):21478–81. [PubMed: 7691811]
16. Schlessinger J, Mohammadi M, Margolis B, Ullrich A. Role of SH2-containing proteins in cellular signaling by receptor tyrosine kinases. *Cold Spring Harb Symp Quant Biol.* 1992; 57:67–74. [PubMed: 1339705]
17. Agazie YM, Hayman MJ. Molecular mechanism for a role of SHP2 in epidermal growth factor receptor signaling. *Mol Cell Biol.* 2003 Nov; 23(21):7875–86. [PubMed: 14560030]

18. Baldys A, Goos M, Morinelli TA, Lee MH, Raymond JR Jr, Luttrell LM, et al. Essential role of c-Cbl in amphiregulin-induced recycling and signaling of the endogenous epidermal growth factor receptor. *Biochemistry*. 2009 Feb 24; 48(7):1462–73. [PubMed: 19173594]
19. Bollag G, McCormick F. Differential regulation of rasGAP and neurofibromatosis gene product activities. *Nature*. 1991 Jun 13; 351(6327):576–9. [PubMed: 1904555]
20. Ekman S, Thuresson ER, Heldin CH, Ronnstrand L. Increased mitogenicity of an alphabeta heterodimeric PDGF receptor complex correlates with lack of RasGAP binding. *Oncogene*. 1999 Apr 15; 18(15):2481–8. [PubMed: 10229199]
21. Jiang X, Sorkin A. Epidermal growth factor receptor internalization through clathrin-coated pits requires Cbl RING finger and proline-rich domains but not receptor polyubiquitylation. *Traffic*. 2003 Aug; 4(8):529–43. [PubMed: 12839496]
22. Pamonsinlapatham P, Hadj-Slimane R, Lepelletier Y, Allain B, Toccafondi M, Garbay C, et al. P120-Ras GTPase activating protein (RasGAP): a multi-interacting protein in downstream signaling. *Biochimie*. 2009 Mar; 91(3):320–8. [PubMed: 19022332]
23. Scheffzek K, Ahmadian MR, Kabsch W, Wiesmuller L, Lautwein A, Schmitz F, et al. The Ras-RasGAP complex: structural basis for GTPase activation and its loss in oncogenic Ras mutants. *Science*. 1997 Jul 18; 277(5324):333–8. [PubMed: 9219684]
24. Beguinot L, Lyall RM, Willingham MC, Pastan I. Down-regulation of the epidermal growth factor receptor in KB cells is due to receptor internalization and subsequent degradation in lysosomes. *Proc Natl Acad Sci U S A*. 1984 Apr; 81(8):2384–8. [PubMed: 6326124]
25. Helin K, Beguinot L. Internalization and down-regulation of the human epidermal growth factor receptor are regulated by the carboxyl-terminal tyrosines. *J Biol Chem*. 1991 May 5; 266(13):8363–8. [PubMed: 2022652]
26. Sorkin A, Di Fiore PP, Carpenter G. The carboxyl terminus of epidermal growth factor receptor/erbB-2 chimerae is internalization impaired. *Oncogene*. 1993 Nov; 8(11):3021–8. [PubMed: 8105439]
27. Sorkin A, Goh LK. Endocytosis and intracellular trafficking of ErbBs. *Exp Cell Res*. 2009 Feb 15; 315(4):683–96. [PubMed: 19278030]
28. Huang G, Chantray A, Epstein RJ. Overexpression of ErbB2 impairs ligand-dependent downregulation of epidermal growth factor receptors via a post-transcriptional mechanism. *J Cell Biochem*. 1999 Jul 1; 74(1):23–30. [PubMed: 10381258]
29. Worthylake R, Opresko LK, Wiley HS. ErbB-2 amplification inhibits down-regulation and induces constitutive activation of both ErbB-2 and epidermal growth factor receptors. *J Biol Chem*. 1999 Mar 26; 274(13):8865–74. [PubMed: 10085130]
30. Zhou X, Agazie YM. The signaling and transformation potency of the overexpressed HER2 protein is dependent on the normally-expressed EGFR. *Cell Signal*. 2012 Jan; 24(1):140–50. [PubMed: 21911055]
31. Hendriks BS, Wiley HS, Lauffenburger D. HER2-mediated effects on EGFR endosomal sorting: analysis of biophysical mechanisms. *Biophys J*. 2003 Oct; 85(4):2732–45. [PubMed: 14507736]
32. Muthuswamy SK, Gilman M, Brugge JS. Controlled dimerization of ErbB receptors provides evidence for differential signaling by homo- and heterodimers. *Mol Cell Biol*. 1999 Oct; 19(10):6845–57. [PubMed: 10490623]
33. Jiang X, Huang F, Marusyk A, Sorkin A. Grb2 regulates internalization of EGF receptors through clathrin-coated pits. *Mol Biol Cell*. 2003 Mar; 14(3):858–70. [PubMed: 12631709]
34. Sun J, Pedersen M, Bengtsson S, Ronnstrand L. Grb2 mediates negative regulation of stem cell factor receptor/c-Kit signaling by recruitment of Cbl. *Exp Cell Res*. 2007 Nov 1; 313(18):3935–42. [PubMed: 17904548]
35. Longva KE, Blystad FD, Stang E, Larsen AM, Johannessen LE, Madshus IH. Ubiquitination and proteasomal activity is required for transport of the EGF receptor to inner membranes of multivesicular bodies. *J Cell Biol*. 2002 Mar 4; 156(5):843–54. [PubMed: 11864992]
36. Aertgeerts K, Skene R, Yano J, Sang BC, Zou H, Snell G, et al. Structural analysis of the mechanism of inhibition and allosteric activation of the kinase domain of HER2 protein. *J Biol Chem*. May 27; 286(21):18756–65. [PubMed: 21454582]

37. Fan YX, Wong L, Ding J, Spiridonov NA, Johnson RC, Johnson GR. Mutational activation of ErbB2 reveals a new protein kinase autoinhibition mechanism. *J Biol Chem*. 2008 Jan 18; 283(3): 1588–96. [PubMed: 18039657]
38. Morandell S, Stasyk T, Skvortsov S, Ascher S, Huber LA. Quantitative proteomics and phosphoproteomics reveal novel insights into complexity and dynamics of the EGFR signaling network. *Proteomics*. 2008 Nov; 8(21):4383–401. [PubMed: 18846509]
39. Ono M, Kuwano M. Molecular mechanisms of epidermal growth factor receptor (EGFR) activation and response to gefitinib and other EGFR-targeting drugs. *Clin Cancer Res*. 2006 Dec 15; 12(24):7242–51. [PubMed: 17189395]
40. Fragale A, Tartaglia M, Wu J, Gelb BD. Noonan syndrome-associated SHP2/PTPN11 mutants cause EGF-dependent prolonged GAB1 binding and sustained ERK2/MAPK1 activation. *Hum Mutat*. 2004 Mar; 23(3):267–77. [PubMed: 14974085]
41. Meng S, Chen Z, Munoz-Antonia T, Wu J. Participation of both Gab1 and Gab2 in the activation of the ERK/MAPK pathway by epidermal growth factor. *Biochem J*. 2005 Oct 1; 391(Pt 1):143–51. [PubMed: 15952937]
42. Ravichandran KS, Lorenz U, Shoelson SE, Burakoff SJ. Interaction of Shc with Grb2 regulates the Grb2 association with mSOS. *Ann N Y Acad Sci*. 1995 Sep 7. 766:202–3. [PubMed: 7486657]
43. Russo C, Dolcini V, Salis S, Venezia V, Violani E, Carlo P, et al. Signal transduction through tyrosine-phosphorylated carboxy-terminal fragments of APP via an enhanced interaction with Shc/Grb2 adaptor proteins in reactive astrocytes of Alzheimer's disease brain. *Ann N Y Acad Sci*. 2002 Nov. 973:323–33. [PubMed: 12485888]
44. Schulze WX, Deng L, Mann M. Phosphotyrosine interactome of the ErbB-receptor kinase family. *Mol Syst Biol*. 2005; 1:2005 0008. [PubMed: 16729043]
45. Monsey J, Shen W, Schlesinger P, Bose R. Her4 and Her2/neu tyrosine kinase domains dimerize and activate in a reconstituted in vitro system. *J Biol Chem*. Mar 5; 285(10):7035–44. [PubMed: 20022944]
46. Zhang X, Gureasko J, Shen K, Cole PA, Kuriyan J. An allosteric mechanism for activation of the kinase domain of epidermal growth factor receptor. *Cell*. 2006 Jun 16; 125(6):1137–49. [PubMed: 16777603]
47. Yamanashi Y, Tezuka T, Yokoyama K. Activation of receptor protein-tyrosine kinases from the cytoplasmic compartment. *J Biochem*. Apr; 151(4):353–9. [PubMed: 22343747]
48. Zhou X, Agazie YM. Molecular mechanism for SHP2 in promoting HER2-induced signaling and transformation. *J Biol Chem*. 2009 May 1; 284(18):12226–34. [PubMed: 19261604]
49. Sperka T, Geissler KJ, Merkel U, Scholl I, Rubio I, Herrlich P, et al. Activation of Ras requires the ERM-dependent link of actin to the plasma membrane. *PLoS One*. 6(11):e27511. [PubMed: 22132106]
50. Lee-Hoeflich ST, Crocker L, Yao E, Pham T, Munroe X, Hoeflich KP, et al. A central role for HER3 in HER2-amplified breast cancer: implications for targeted therapy. *Cancer Res*. 2008 Jul 15; 68(14):5878–87. [PubMed: 18632642]
51. Rana P, Sridhar SS. Efficacy and tolerability of lapatinib in the management of breast cancer. *Breast Cancer (Auckl)*. 6:67–77. [PubMed: 22438669]
52. Debnath J, Muthuswamy SK, Brugge JS. Morphogenesis and oncogenesis of MCF-10A mammary epithelial acini grown in three-dimensional basement membrane cultures. *Methods*. 2003 Jul; 30(3):256–68. [PubMed: 12798140]
53. Agazie YM, Movilla N, Ischenko I, Hayman MJ. The phosphotyrosine phosphatase SHP2 is a critical mediator of transformation induced by the oncogenic fibroblast growth factor receptor 3. *Oncogene*. 2003 Oct 9; 22(44):6909–18. [PubMed: 14534538]
54. Yuan YL, Zhou XH, Song J, Qiu XP, Li J, Ye LF. Dual silencing of type 1 insulin-like growth factor and epidermal growth factor receptors to induce apoptosis of nasopharyngeal cancer cells. *J Laryngol Otol*. 2008 Sep; 122(9):952–60. [PubMed: 17908353]
55. Duan L, Miura Y, Dimri M, Majumder B, Dodge IL, Reddi AL, et al. Cbl-mediated ubiquitinylation is required for lysosomal sorting of epidermal growth factor receptor but is dispensable for endocytosis. *J Biol Chem*. 2003 Aug 1; 278(31):28950–60. [PubMed: 12754251]

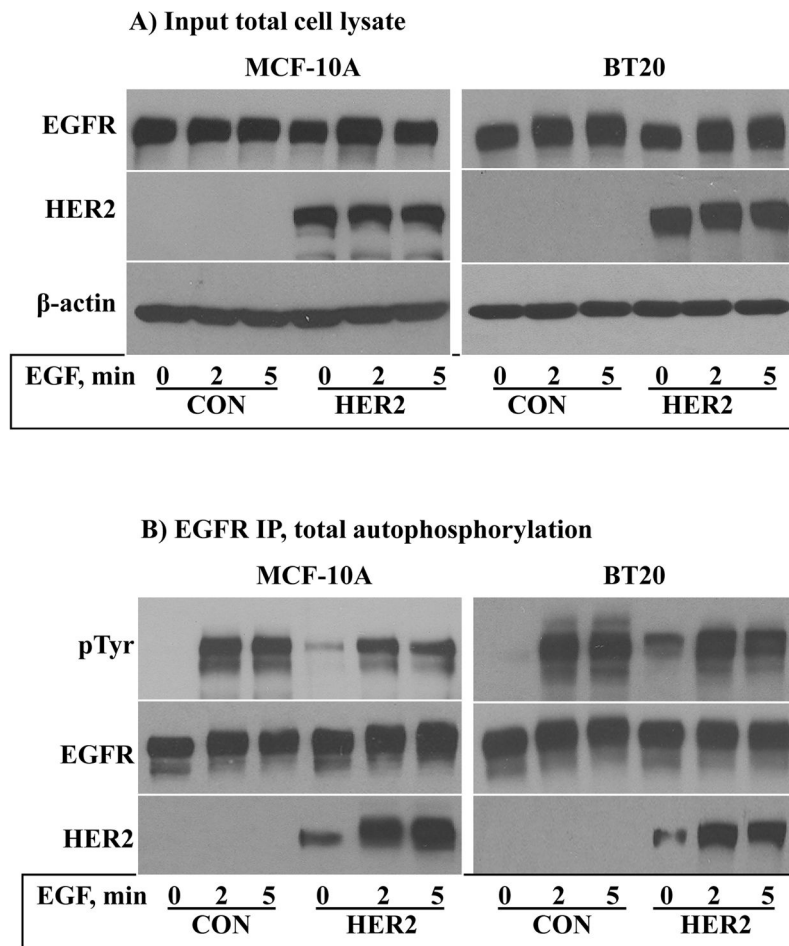


Figure 1A and B

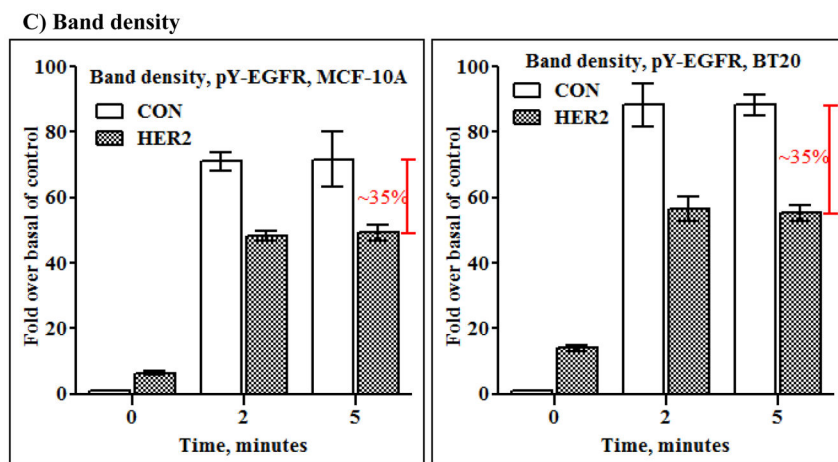


Figure 1C

Figure 1.

Analysis of EGF-induced receptor autophosphorylation. The control and the HER2 cells derived from the MCF-10A and the BT20 lines were serum starved overnight and then stimulated with EGF (10 ng/ml) for 2 minutes, 5 minutes or left unstimulated. A) Input total cell lysate analysis for EGFR and HER2 in the MCF-10A breast epithelial and in the BT20 breast cancer cell lines. HER2 was expressed in both cells by retrovirus-mediated transduction. The expression of EGFR in all lanes and HER2 in the corresponding lanes was comparable. B) EGFR was immunoprecipitated from the total cell lysates shown in A, and then analyzed for total autophosphorylation by immunostaining with anti-pY antibody. Reblotting with anti-EGFR and anti-HER2 antibodies showed that EGFR was successfully precipitated, and HER2 was likewise co-precipitated in the expected lanes. C) Band density measurement of anti-pY blots of EGFR in the controls, and EGFR and HER2 heterodimers in the HER2 cells. The results shown were mean \pm S.D. (standard deviation) taken from three independent experiments.

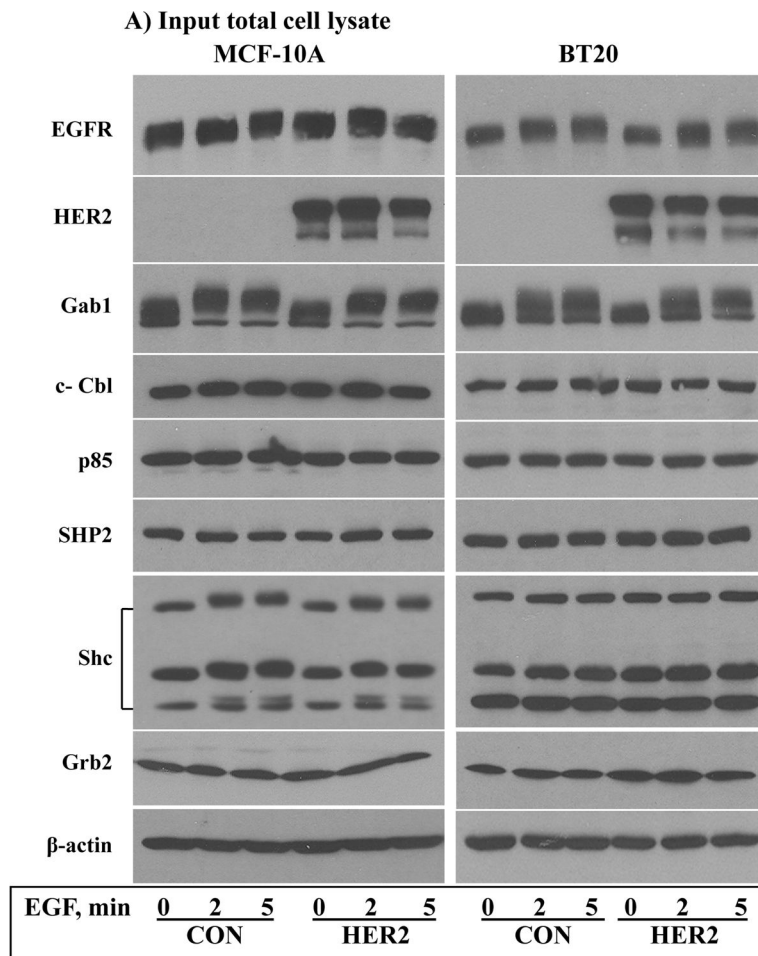


Figure 2A

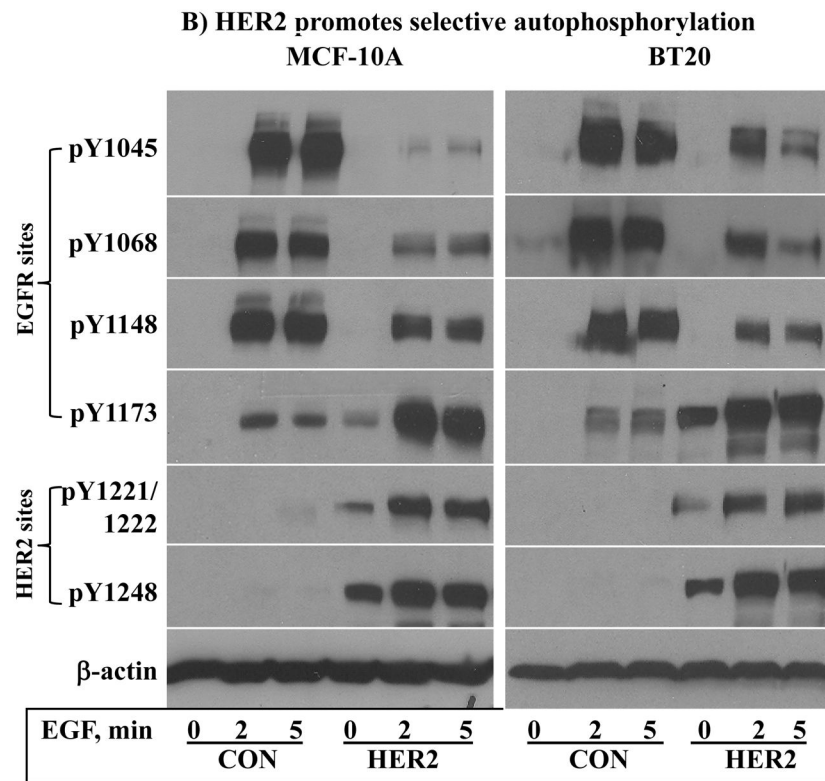


Figure 2B

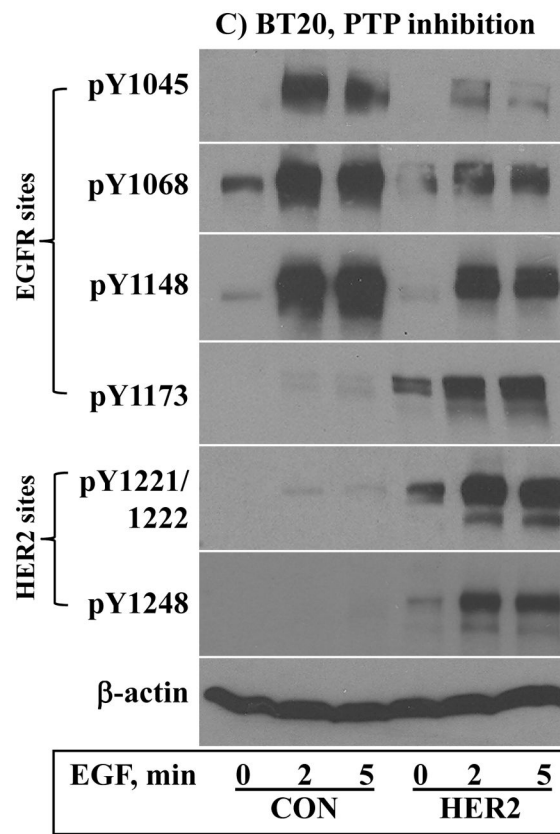


Figure 2C

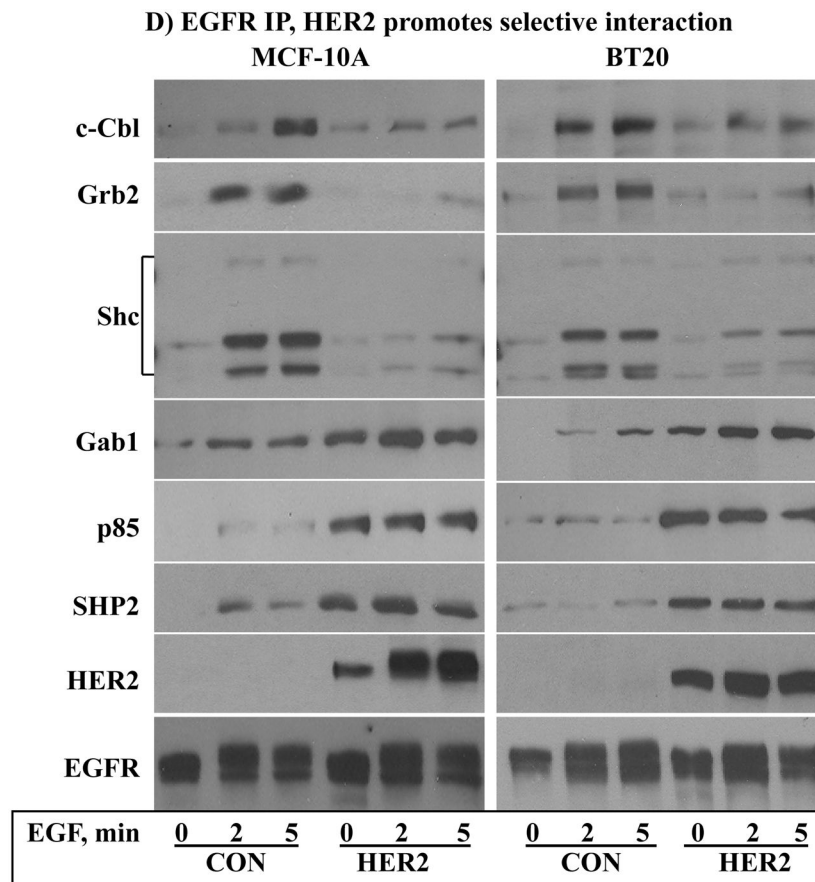


Figure 2D

Figure 2.

Analysis of specific autophosphorylation and interaction. The control and the HER2 cells were serum starved overnight and then stimulated with EGF (10 ng/ml) for the indicated time points. A) Input total cell lysate analysis for EGFR, HER2, Gab1, c-Cbl, p85 (PI3K), SHP2, Shc, Grb2 and β -actin (loading control). B) Analysis of individual autophosphorylation sites in EGFR and HER2 using phospho-specific antibodies. In this study, four EGFR and three HER2 autophosphorylation sites were analyzed. C) Effect of PTP inhibition on receptor autophosphorylation patten. Cells were treated with 1 mM orthovanadate for 30 minutes prior to EGF stimulation. Lysates prepared from these cells were analyzed for EGFR and HER2 autophosphorylation as shown. D) Immunoprecipitation and immunostaining analysis of c-Cbl, Grb2, Shc, Gab1, p85 (PI3K) and SHP2 interaction with EGFR and EGFR:HER2. Note that the interaction of Grb2 and Shc was higher in the control cells and lower in the HER2 cells, and the opposite was true for Gab1, p85 (PI3K) and SHP2.

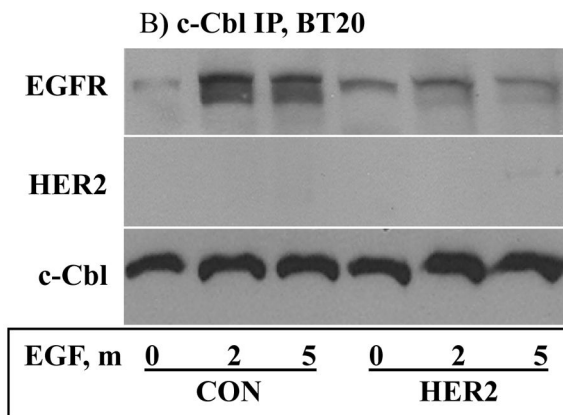
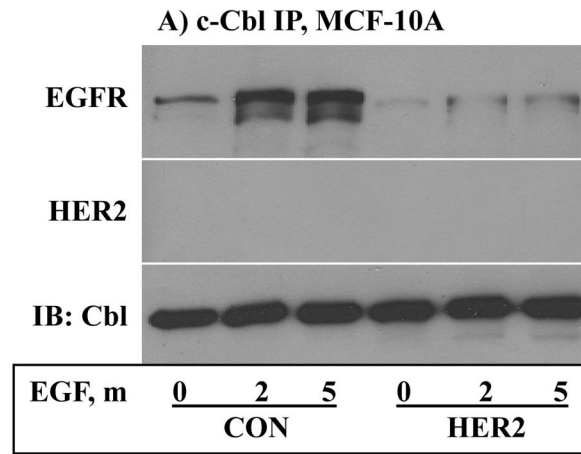


Figure 3A and B

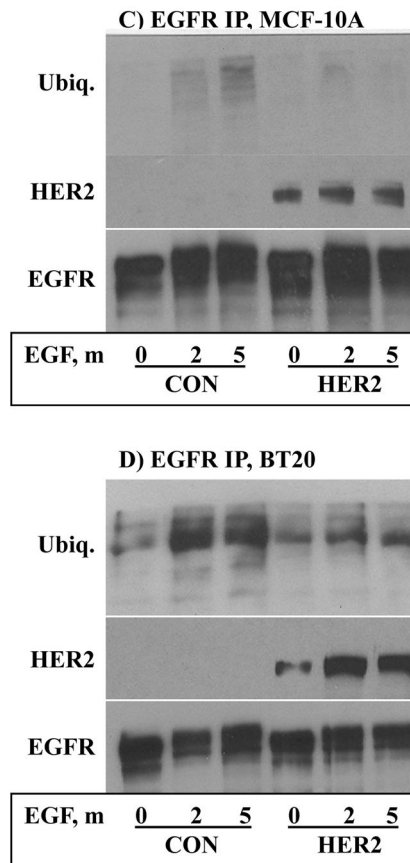


Figure 3C and D

Figure 3.

Analysis of EGFR and HER2 coprecipitation with c-Cbl in the MCF-10A (A) and BT20 (B) cell lines. The control and the HER2 cells were serum starved overnight and then stimulated with EGF (10 ng/ml) for the indicated time points. Lysates prepared from these cells were subjected to anti-Cbl immunoprecipitation, and then to immunostaining with the indicated antibodies. State of receptor ubiquitylation (top), HER2 and EGFR coprecipitation (middle and bottom, respectively) were analyzed by immunostaining with specific antibodies. Data from the MCF-10A is shown in C while from the BT20 in D.

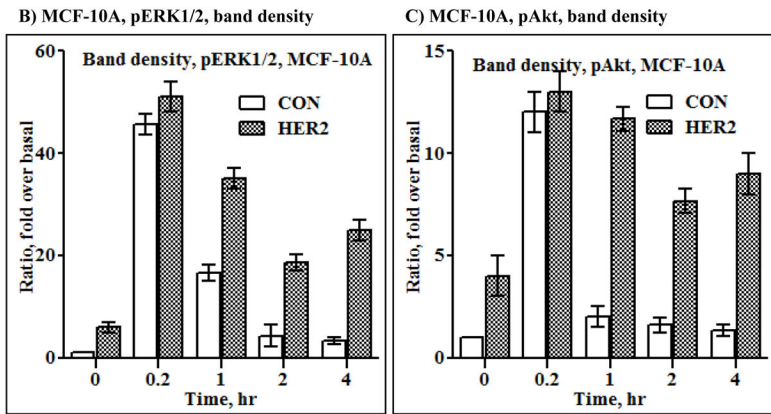
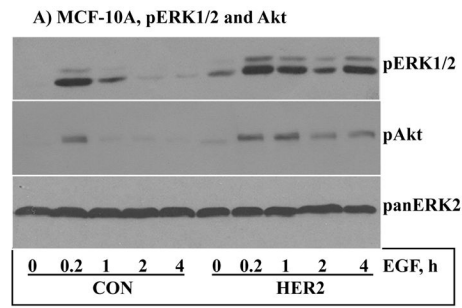


Figure 4A, B and C

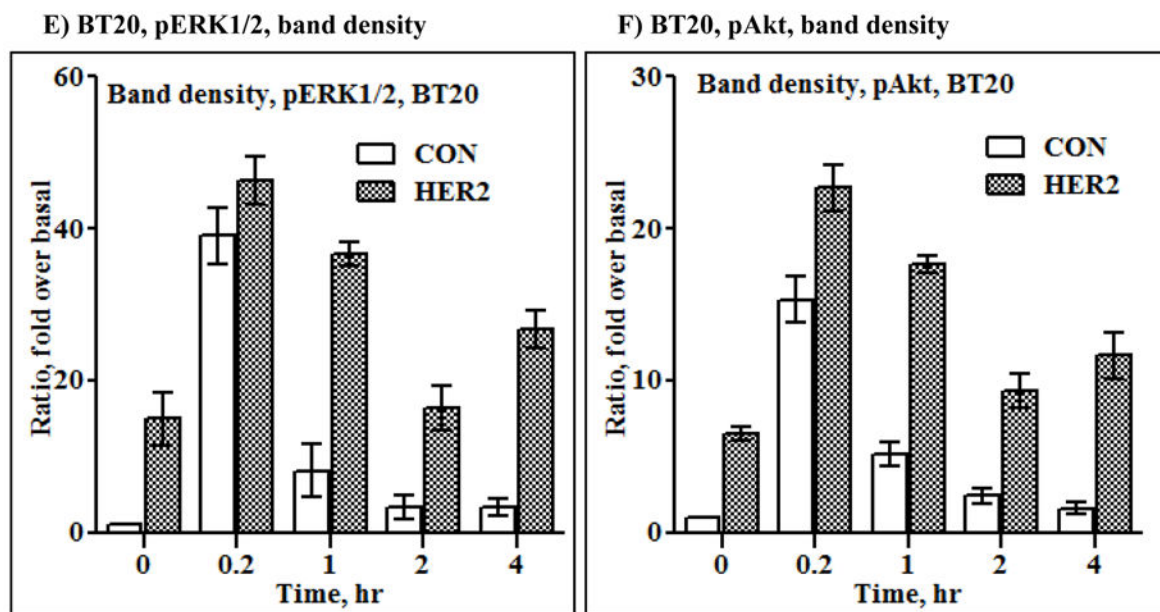
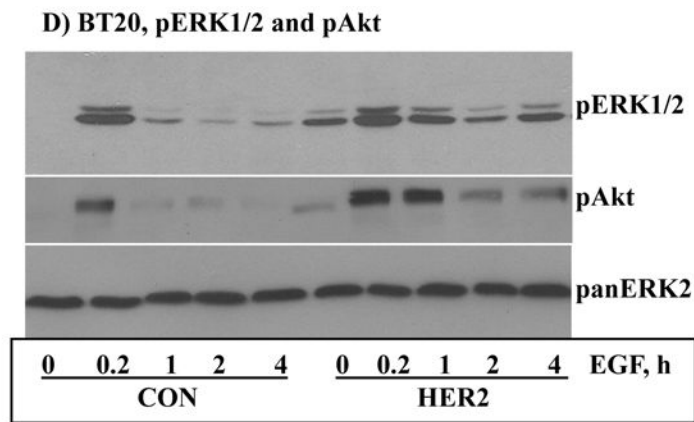
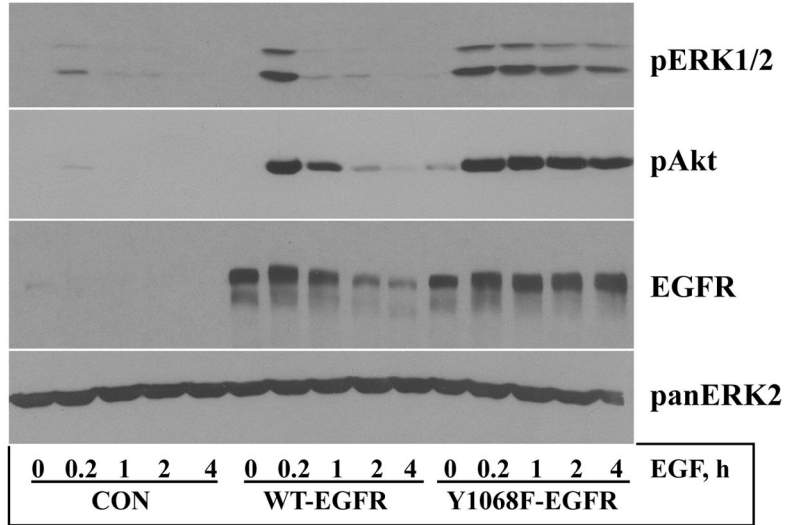


Figure 4D, E and F

Figure 4.

Impact of HER2 expression on signaling. As compared to the controls, expression of HER2 led to an enhanced and sustained ERK1/2 and Akt activation in both the MCF-10A (A) and BT20 (D) lines. Band density analysis of ERK1/2 and Akt activation in the MCF-10A- (B and C) and BT20- (E and F) derived lines showed short-lived signaling in the controls and sustained signaling with slight decline and revamp in the HER2 cells. Basal pERK1/2 and pAkt activation levels (no EGF stimulation) in the controls were used as reference to calculate “fold over basal”. The results shown are averages of three independent experiments \pm S.D. (standard deviation).

A) Signaling by WT-EGFR and Y1068F-EGFR



B) Signaling by WT-HER2 and Y1139F-HER2

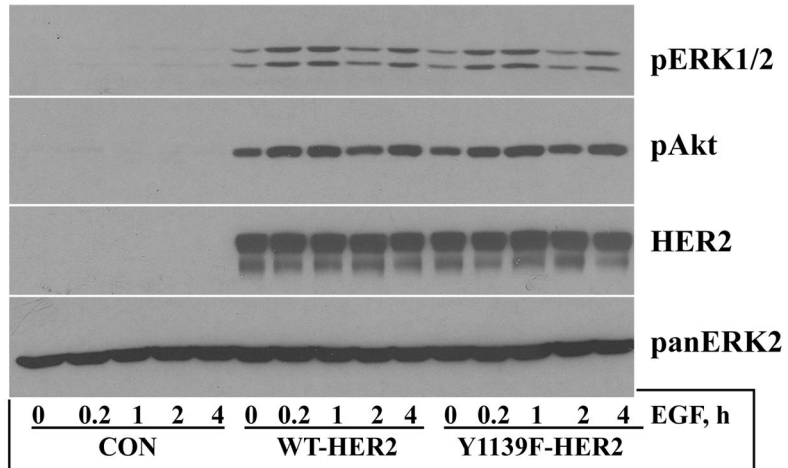
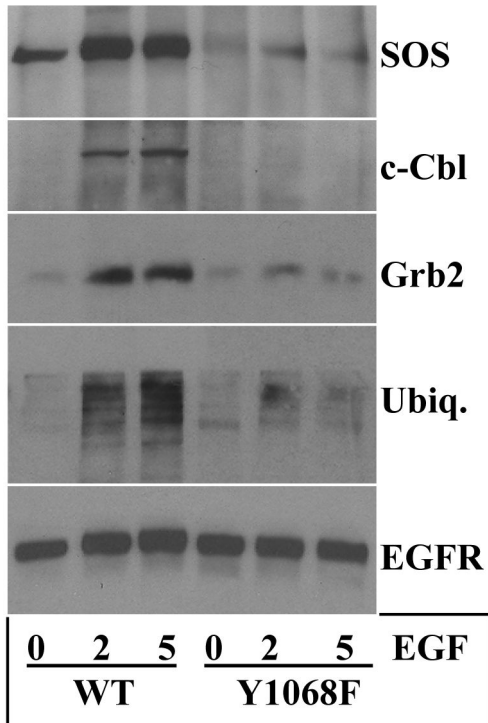
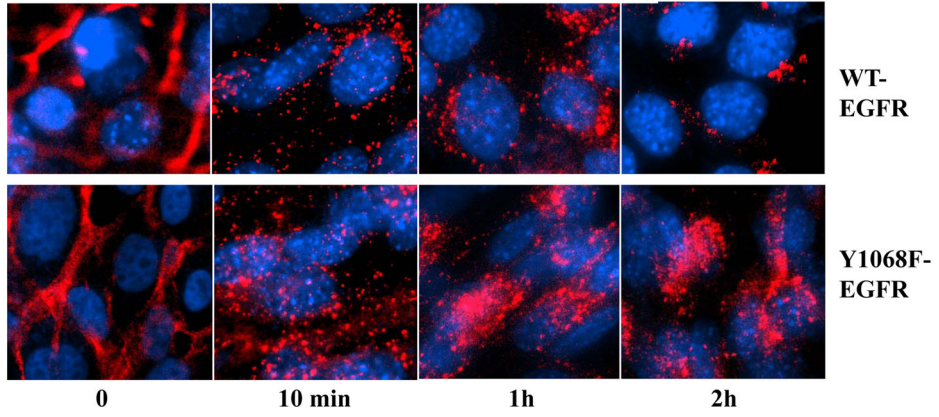


Figure 5A and B

C) FLAG IP for EGFR**Figure 5C**

D) MEF-EGFR, TRITC-EGF fluorescence , 40× objective



E) MCF-10A, TRITC-EGF fluorescence, 40× objective

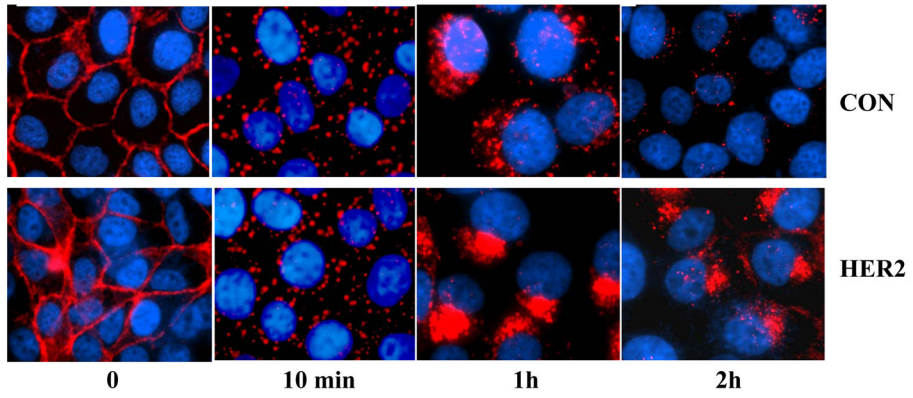


Figure 5D and E

F) BT20, TRITC-EGF fluorescence, 40× objective

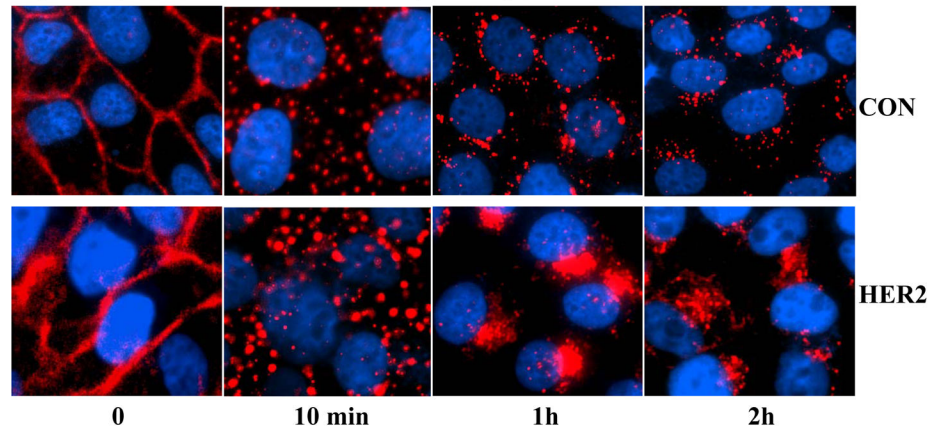
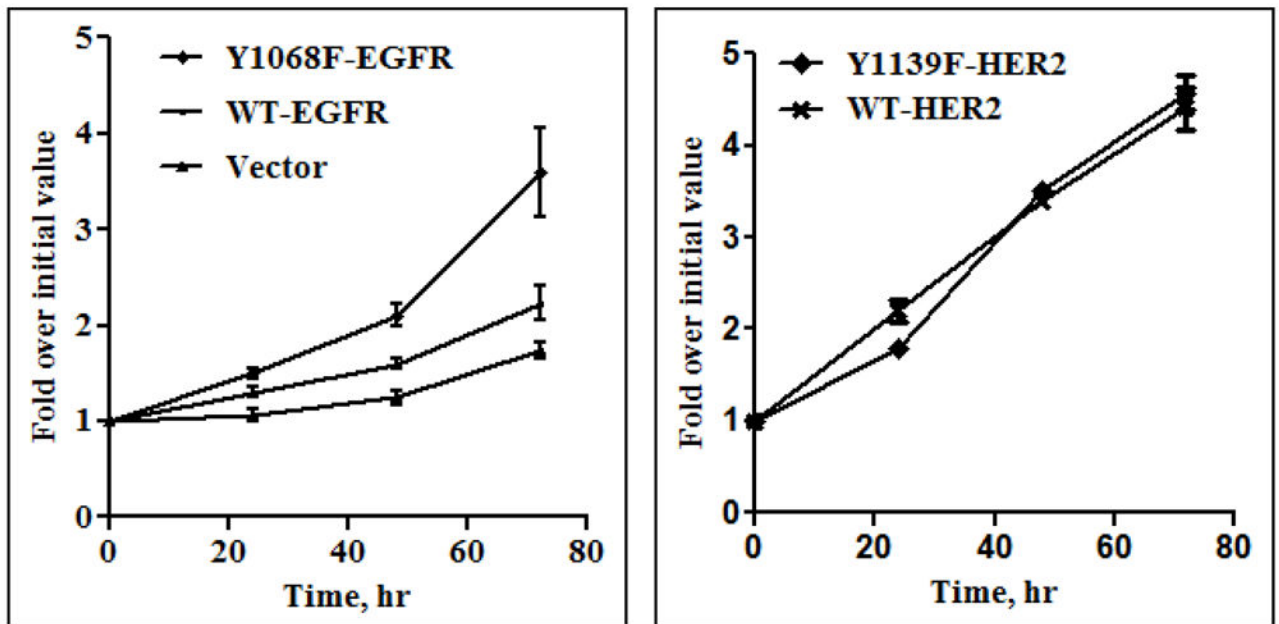


Figure 5F

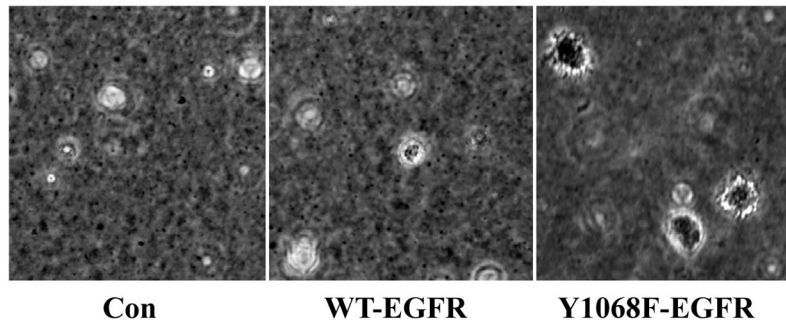
Figure 5.

Mutation of the Grb2 binding site in EGFR and HER2 does not perturb signaling. A) Vector, WT-EGFR or Y1068F-EGFR were expressed in the mouse embryo fibroblast (MEF) cells by retroviral transduction, and their impact on EGF-induced ERK1/2 and Akt activation was analyzed by immunostaining with specific antibodies. Anti-EGFR immunostaining showed that the expression of both EGFR proteins was comparable. Note also that Y1068F-EGFR is resistant to EGF-induced degradation. B) Similarly, the vector and the WT-HER2 and the Y1139F-HER2 proteins were expressed in MEFs and analyzed for ERK1/2 and Akt activation and HER2 expression. Note that both WT-HER2 and Y1139F-HER2 induce constitutive signaling, and their stability was unaffected by EGF stimulation. C) Interaction of SOS, Grb2 and c-Cbl with EGFR proteins and state EGFR ubiquitylation were analyzed by immunoprecipitation with anti-FLAG and immunostaining with the indicated antibodies. D) Dynamics of EGF-induced WT-EGFR and Y1068F-EGFR processing in MEFs. Also shown in E and F are dynamics of EGF-induced EGFR (endogenous) processing in the MCF-10A and BT20 lines, respectively. For fluorescence studies, cells were serum-starved overnight, chilled at 4°C for 1 hour, treated with 10 ng/ml TRITC-labeled EGF at 4°C for 1 hour, transferred to 37°C and incubated for the indicated time points. Preparation of coverslips and picture collection was as described in the materials and methods.

A) Cell growth rate, MEFs



B) EGFR on anchorage-independent growth, 5× objective



C) HER2 on anchorage-independent growth, 5× objective

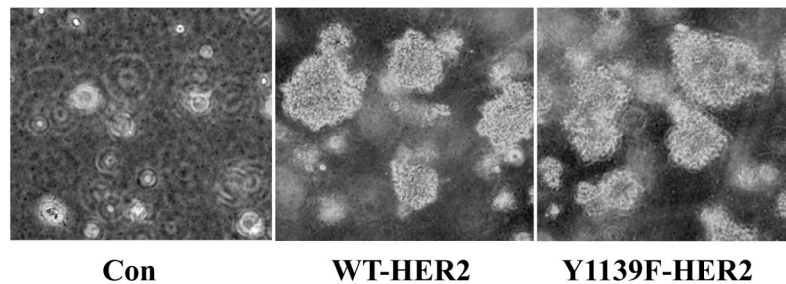
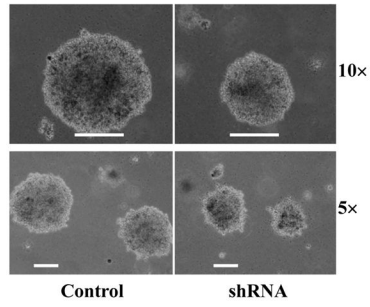
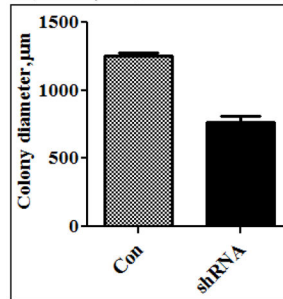


Figure 6B and C

D) Colonies in Skbr-3 cells



E) Colony size, Skbr-3 cells



F) Colony number, Skbr-3 cells

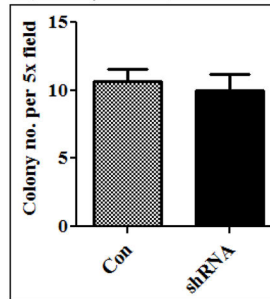
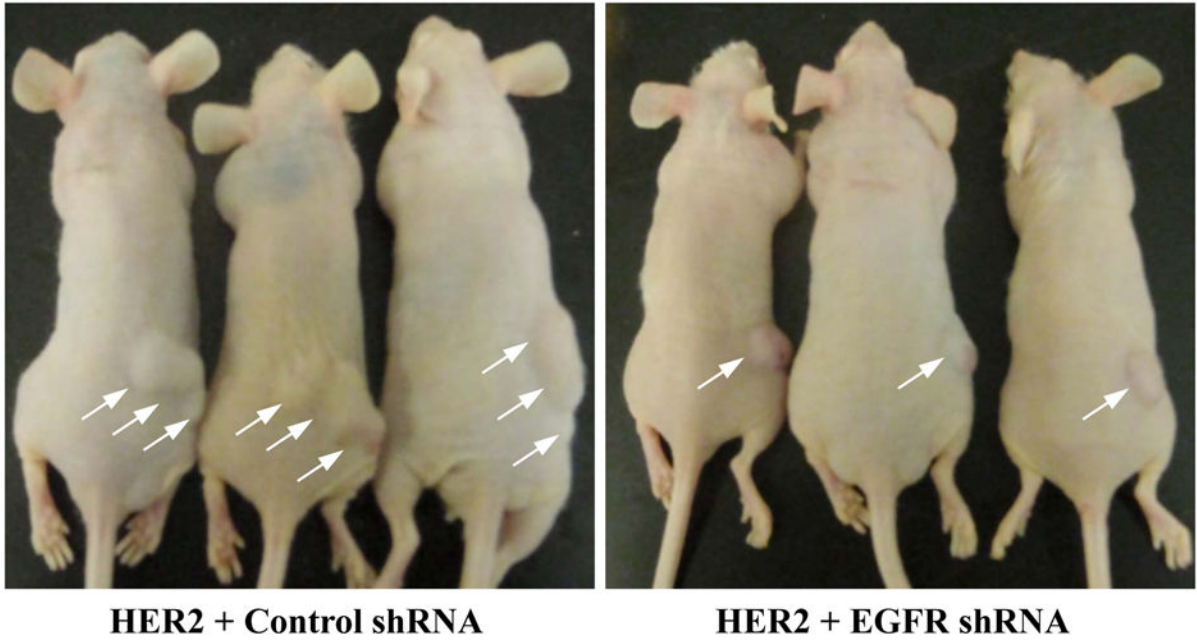


Figure 6D, E and F

G) Xenograft tumor growth in nude mice



H) Isolated tumors

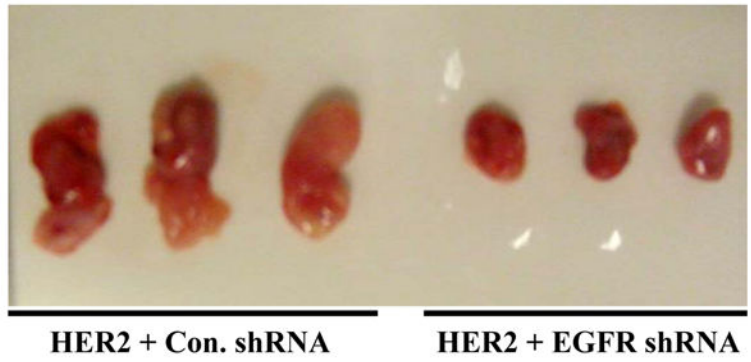


Figure 6G and H

I) Analysis of tumor weight

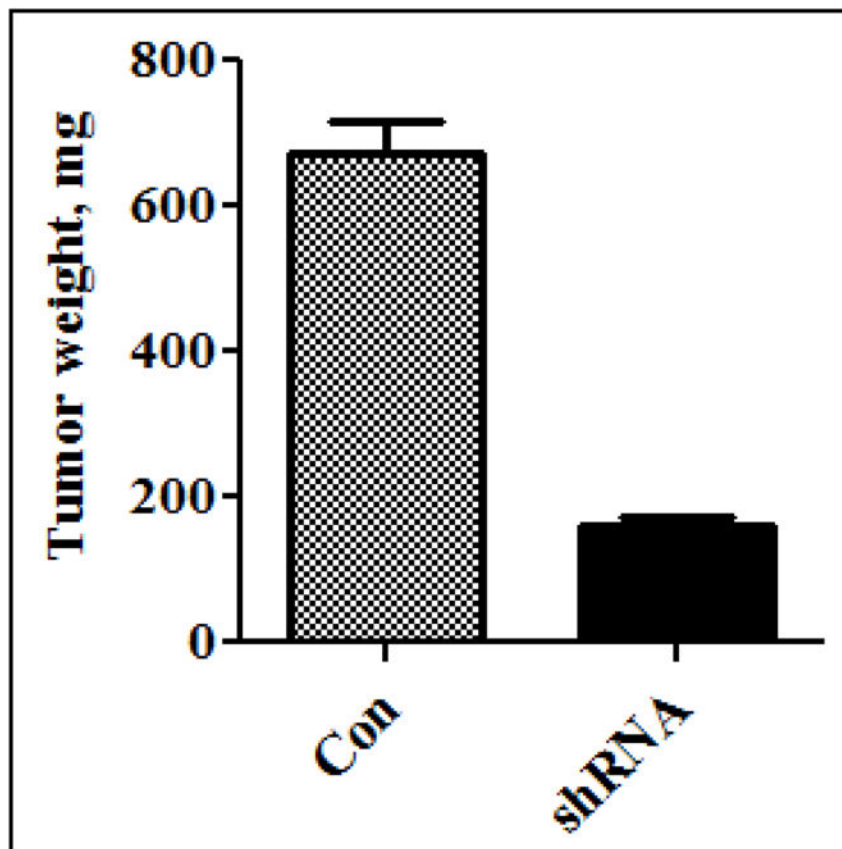


Figure 6.

A) Impact of EGFR (left) and HER2 (right) expression on cell proliferation was determined by counting cells in 10 random 4x objective fields and then averaging. The results shown are mean \pm S.D. (standard deviation) of three independent experiments. B) Expression of Y1068F-EGFR, but not WT-EGFR in MEFs induced colony formation in soft agar in the presence of 2 ng/ml EGF. C) Expression of both WT-HER2 and Y1139F-HER2 in MEFs induced robust colony formation in soft agar. D) Pictures of colonies, one at 10 \times and another at 5 \times objectives for each group, showing effect of EGFR silencing on colony formation by the Skbr-3 HER2-positive breast cells. Scale bar represents 500 μ m. E) Bar graph showing differences in colony size formed by the control and EGFR-shRNA cells after 10 days of incubation in soft agar. F) Bar graph showing colony number as determined by counting 10 random fields under 4 \times objective and then averaging; data shown is mean \pm S.D. (standard deviation) of three independent experiments. G) Pictures of mice bearing xenograft tumors initiated by subcutaneous injection of $\sim 10^6$ BT20-HER2 cells expressing control or EGFR-specific shRNA. Note the differences in size and shape where the shRNA are smaller and relatively rounded while the controls are larger and irregular. H) Pictures of isolated tumors also show differences in size and shape. I) Bar graph showing differences in tumor weight

between the control and the shRNAcells; data shown is average weight of the three tumors in each group \pm S.D. (standard deviation).

Author Manuscript

Author Manuscript

Author Manuscript

Author Manuscript